Available online at www.sciencedirect.com

ScienceDirect

IFAC PapersOnline CONFERENCE PAPER ARCHIVE

IFAC PapersOnLine 52-14 (2019) 60–65

Predicting optimal operating points by modelling different flotation mechanisms ⋆

Daniël J. Oosthuizen *,** **Ian K. Craig** *

* *ProcessIQ, Perth, Australia (e-mail: kobus@processiq.com.au)*
** *University of Pretoria, Pretoria, South Africa (e-mail: ian.craig@up.ac.za)*

Abstract: The inverse relationship between grade and recovery in flotation circuits is well accepted, and forms the basis of control strategies used to maxisise recovery subject to grade specifications. The concept of peak air recovery however suggests that this relationship is more complex, and that a model of this peak could indicate an optimal operating point. In this paper froth stability is modelled using a combination of fundamental and empirical models. Potential applications of a non-linear model in optimising flotation performance investigated, and the benefits demonstrated.

Keywords: Flotation, process optimisation, modelling

1. INTRODUCTION

For a flotation process, an inverse relationship exists between grade and recovery (Wills and Napier-Munn, 2006). Product specifications define a desired grade, while the quantity of product relative to the feed content is defined by the recovery. A common flotation optimisation philosophy is hence to minimise grade subject to the product specification, in order to maximise recovery (Laurila et al., 2002).

The manipulated variables commonly used to influence grade and recovery are the aeration rates to flotation cells, the froth depth and also reagent addition (Bascur and Herbst, 1985). Reagent addition typically occurs at a limited number of addition points – not at each flotation cell. The aeration rates and/or level setpoints of each flotation cell can typically be set individually as manipulated variables.

In control strategies to control grade to setpoint, the effect of variations in aeration rate and level setpoints of each cell on the final grade and recovery is often assumed to be linear (Oosthuizen et al., 2017). Although such a model is useful within a narrow operating region, it does not take the interactions between cells into account, resulting in degraded model accuracy when deviating from the operating point where the model was fitted. It furthermore has limited potential to optimise flotation operation, particularly when non-linear effects such as froth stability plays a significant role. Variations in feed rate or compositions would also affect the model accuracy, resulting in a crude model approximation to optimise an interactive system.

In what follows, it will be shown that, depending on the operating point, optimal operation is not necessarily achieved by adjusting the aeration rates of all cells in the same direction to increase or decrease grade to a value close to specification. Automatic control is often capable of controlling overall grade to setpoint using this approach, but there are multiple solutions yielding the desired grade, and the operating point achieved may not be the optimal operating point.

2. SIMULATION MODEL

The two main flotation mechanisms governing the transfer of material between the pulp and froth phases, are the true flotation of hydrophobic particles, and entrainment of all particles together with the bubble stream (Wills and Napier-Munn, 2006). True flotation is often modelled as a first order process, while entrainment is a function of particle size and density, as well as the upward stream of liquid (water recovery) as part of the bubble stream.

Oosthuizen and Craig (2018) showed how the use of a floatability distribution instead of a single flotation constant improves model accuracy. The same holds for entrainment, as particle size and density has a large impact on the likeliness of a particle being entrained. For this simulation study, Platinum group metals (PGMs), Chromite and Gangue were modelled and 100 size classes were defined for each specie, distributed over the size range between $8\mu m$ and $220\mu m$, as shown by Harris (2000).

2.1 True Flotation model

The core of the model is a kinetic model, based on a chemical reactor analogy, as described by Polat and Chander (2000) for a batch reactor. Such a model has the general form:

$$\frac{dC_p(t)}{dt} = -K(t) \cdot C_p(t) \cdot C_b(t) \tag{1}$$

where C_p and C_b represent the concentrations of particles and bubbles at time t respectively. $K(t)$ is a pseudo rate-

⋆ This work is based on research supported in part by the National Research Foundation of South Africa (Grant number 111741).

10.1016/j.ifacol.2019.09.164

constant that depends on various parameters affecting the flotation process, and may vary with time. For this study, $K(t)$ will not be time variable, but will be a distribution with different values for each size class. This equation describes the change in concentration in any species in the flotation vessel due to material transfer between the slurry and froth phases.

As the attachment of particles only takes place on the surfaces of bubbles, the effect of bubble surface area flux is taken into account by replacing C_b with a bubble surface area flux term (S_b), as described by Runge and Franzidis (2003).

$$\frac{dC_p(t)}{dt} = -K(t) \cdot C_p(t) \cdot S_b(t) \tag{2}$$

The bubble surface-area flux calculation, S_b, in (2) can be calculated using (3), with J_g the superficial gas velocity, and D_{32} the Sauter mean bubble diameter. J_g is calculated from the aeration rate of the flotation cell and its surface area.

$$S_b = 6\frac{J_g}{D_{32}} \tag{3}$$

2.2 Water recovery model

Neethling and Cilliers (2009) derived an equation for water recovery based on fundamental models, and showed for a two-phase system (Neethling et al., 2003) that froth depth or froth residence time is not the main cause of reduced water recovery observed when froth height increase (Wang et al., 2016; Zheng et al., 2006), but rather the increase in bubble size associated with deep froths. Neethling et al. (2003) showed that water recovery has an inverse squared relation to bubble-diameter, with the proportionality constant determined by the bubble shape.

The model for water-recovery is shown in (4), for Q_w the volumetric water flow, A_{col} the cross-sectional area of the froth column, α the air-recovery (between zero and one) and λ_{out} the Plateau border length per volume of froth. Equation (6) shows the Plateau border length, assuming that the bubbles have similar geometry as Kelvin cells (Neethling et al., 2003). k_1 gives the balance between gravity and viscosity, with ρ the liquid density, C_{PB} the plateau border drag coefficient, and μ the fluid viscosity.

$$if \alpha < 0.5 : \frac{Q_w}{A_{col}} = \frac{{J_g}^2 \cdot \lambda_{out}}{k_1} \cdot (1-\alpha) \cdot \alpha \tag{4}$$

$$if \alpha \geq 0.5 : \frac{Q_w}{A_{col}} = \frac{{J_g}^2 \cdot \lambda_{out}}{4k_1} \tag{5}$$

$$\lambda_{out} \approx \frac{6.81}{{D_{32}}^2} \tag{6}$$

$$k_1 = \frac{\rho g}{3C_{PB} \cdot \mu} \tag{7}$$

The use of a fundamental model is preferred over an empirical model, as the effect of other disturbances can easily be integrated into such a model by considering their effect on the fundamental properties. The effect of entrained particles on the liquid viscosity can for example be integrated into the model described above by including this effect into (7).

2.3 Entrainment model

Neethling and Cilliers (2009)'s entrainment model uses the change in liquid velocity in the froth due to large changes in bubble size with froth height as a key component of the model. The particle settling velocity, v_{set}, describes the effect of particle size (d_p) and density (ρ_s) on entrainment, with g the constant of gravitational acceleration.

$$v_{set} \approx \frac{1}{3}\frac{g \cdot (\rho_s - \rho) \cdot d_p^2}{18\mu} \tag{8}$$

The axial dispersion coefficient, D_{Axial}, is given below, k_1 is defined in (7), providing the balance between gravity and viscosity, and Pe is the Peclet number.

$$D_{Axial} \approx \frac{J_g^{1.5}}{\sqrt{k_1\left(\sqrt{3} - \pi/2\right)Pe}} \tag{9}$$

v_{set} and D_{Axial} are finally included in a simplified equation for entrainment, taking the bubble-size at which the liquid velocity equals the settling velocity into account (Neethling and Cilliers, 2009). h_{froth} refers to the froth depth.

$$if \alpha < 0.5 : Ent \approx exp\left(-\frac{v_{set}^{1.5} \cdot h_{froth}}{D_{Axial}\sqrt{J_g \alpha(1-\alpha)}}\right) \tag{10}$$

$$if \alpha \geq 0.5 : Ent \approx exp\left(-\frac{2v_{set}^{1.5} \cdot h_{froth}}{D_{Axial}\sqrt{J_g}}\right) \tag{11}$$

Note that these equations are only valid for the ranges shown below.

$$if \alpha < 0.5 : 0 \leq \frac{\sqrt{v_{set}}}{\sqrt{J_g \alpha(1-\alpha)}} \leq 1 \tag{12}$$

$$if \alpha \geq 0.5 : 0 \leq \frac{2\sqrt{v_{set}}}{\sqrt{J_g}} \leq 1 \tag{13}$$

In the simplest version of Neethling and Cilliers (2009)'s entrainment model, the term relating bubble diameter at the froth-pulp interface relative to the bubble diameter at the top of froth was ignored, as the significant increase in bubble size between the bottom and top of the froth layer makes this term negligible under most operating conditions.

For control purposes, and specifically for shallow froth layers where this assumption does not hold, the effect of variations in froth residence time (through variations in aeration rate and froth level) on bubble diameter can be accounted for by including this term. A suitable model of variation in bubble size with residence time, as well as the variation in bubble size at the froth-pulp interface with J_g would be required. Although both J_g and h_{froth} already forms part of the entrainment models defined in (10) and

(11), and given that this is already a simplified model, the buble size at the top of the froth layer needs to be modelled for the water recovery model, and will hence be included, by reverting to an intermediate simplification provided by Neethling and Cilliers (2009), where r_{in} and r_{out} refers to the bubble sizes at the bottom- and top of the froth respectively.

$$if \alpha < 0.5$$
$$Ent \approx exp\left(-\frac{v_{set}}{D_{Axial}} \cdot h_{froth} \cdot \frac{\sqrt{\frac{v_{set}}{J_g \alpha(1-\alpha)}} - \frac{r_{in}}{r_{out}}}{(1-\frac{r_{in}}{r_{out}})}\right) \quad (14)$$

$$if \alpha \geq 0.5$$
$$Ent \approx exp\left(-\frac{v_{set}}{D_{Axial}} \cdot h_{froth} \cdot \frac{\sqrt{\frac{4v_{set}}{J_g}} - \frac{r_{in}}{r_{out}}}{(1-\frac{r_{in}}{r_{out}})}\right) \quad (15)$$

These two equations are only valid for the ranges:

$$if \alpha < 0.5 : 0 \leq \frac{\sqrt{\frac{v_{set}}{J_g \alpha(1-\alpha)}} - \frac{r_{in}}{r_{out}}}{(1-\frac{r_{in}}{r_{out}})} \leq 1 \quad (16)$$

$$if \alpha \geq 0.5 : 0 \leq \frac{\sqrt{\frac{4v_{set}}{J_g}} - \frac{r_{in}}{r_{out}}}{(1-\frac{r_{in}}{r_{out}})} \leq 1 \quad (17)$$

2.4 Froth Stability model

Several attempts have been made to model froth stability and the effect of the entrained and attached particles on froth stability – often with conflicting results (Ata (2008), Tang and Tan (1989)). A simplified model have also been used, based on an experimentally determined maximum froth height obtained for the operating conditions considered ($h_{froth-max}$). Zheng et al. (2006) describes a linear relation to estimate the effect of froth height on water recovery as given by (18).

$$\alpha = 1 - \frac{h_{froth}}{h_{froth-max}} \quad (18)$$

Although aspects such as maximum froth height and bubble size is part of the model derivation for the models described above, these are not used in any models for froth stability. Neethling and Brito-Parada (2018) concluded that the mechanisms for froth stability cannot be modelled with sufficient accuracy, and hence used an empirical relation to model froth stability in combination with the fundamental models described earlier. A similar approach is followed in this paper to model froth stability, by including both fundamental aspects such as maximum achievable bubble size, and also an empirical term to model the effect of an increase in turbulence with increasing J_g.

3. EXPERIMENTAL SETUP

The pilot flotation circuit as described by (Harris, 2000) was simulated using the models for true flotation, entrainment and water recovery as described by Neethling and Brito-Parada (2018). The froth stability model described above was integrated with this model. Parameters were adjusted to ensure that the simulator gives similar outputs to the pilot plant results obtained by (Harris, 2000). The aeration rates and cell levels used in the pilot plant tests were used as default operating points. The grade and recovery at the default operating point was used as a reference.

A sweep of aeration rates resulting in J_g between 0 and 2 cm/s were performed, to calculate the peak air recovery values and the aeration rates at which they occur at the default froth depths. These sweeps were repeated at froth depths higher and lower than the default values. The performance of a bank at peak air recovery values were compared to its performance at the default operating point.

It was attempted to find an alternative operating point resulting in the same grade, but occurring at peak air recovery values, by interpolating between the simulated values at froth depths higher and lower than the default operating point. The performance of a bank at this alternative operating point was compared to that at the default operating point.

4. RESULTS

The modelled froth stability (α) for 5 cells in a rougher bank is shown in Fig. 1. At low values of J_g, the froth residence time would be high, resulting in significant growth in bubble sizes due to bubble coalescence. α hence needs to reduce to only allow bubble diameters smaller than the maximum bubble size, which is a function of water recovery. At higher values of J_g, the shape of the trend is dominated by the effect of an increase in turbulence to destabilise the froth. In this study, this was modelled as a linear effect. The difference between the trends for the five cells are mainly due to different froth depths. It can be seen that the values of α is of similar magnitude as the graph shown in Neethling and Brito-Parada (2018), and that the peak occurs in a similar region as the default operating range for the pilot plant study by Harris (2000) (average $J_g = 0.5$ cm/s).

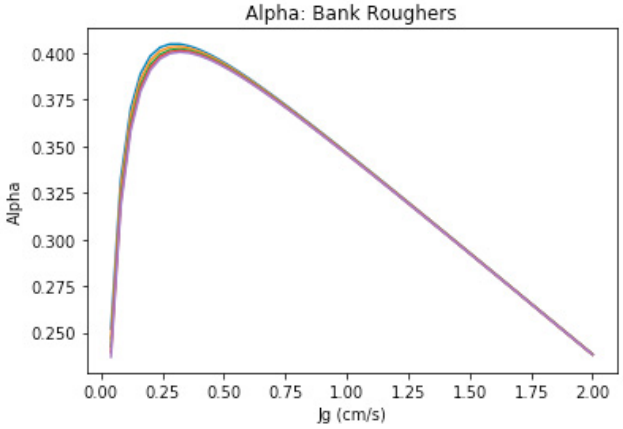

Fig. 1. Froth Stability For 5 Cells

A comparison between the froth stability values for deep, shallow and the default froth depths are shown in Fig. 2. The graphs with peaks at lower values of J_g were for

lower froth depths, and those with peaks at higher values of J_g were for deeper froths. This is consistent with the results reported by Hadler et al. (2012) for test work on an industrial plant. Froth stability plays a key role in the model, as this component allows for optimisation due to the non-linearities it introduces.

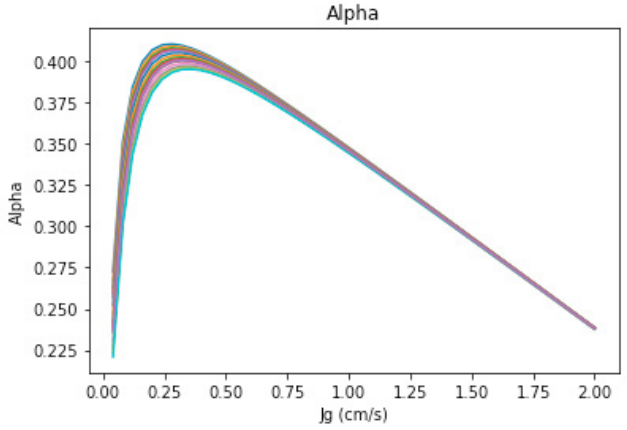

Fig. 2. Comparison of froth stability at different froth depths

The values of J_g at which the peaks in froth stability, α, occur, are tabulated below for different froth depths, together with the default operating point. The resolution of the simulation (50 samples over the range of 2 cm/s) explains why the peaks occur at identical values for some cells in the bank.

Table 1. J_g values at α peaks, compared to default operating point

h_{froth}	J_g	Cell 1	Cell 2	Cell 3	Cell 4	Cell 5
7.8 cm	Default	0.45	0.46	0.51	0.50	0.54
7.8 cm	Peak	0.32	0.32	0.32	0.32	0.32
9.4 cm	Peak	0.32	0.32	0.32	0.36	0.36
6.3 cm	Peak	0.28	0.28	0.28	0.28	0.28

It can be seen that J_g for the default operating point was considerably higher than the values of J_g where the peak in froth stability occurs. It must however be kept in mind that data was not available to fit the peak air recovery curve based on data collected during the original experiment by Harris (2000). The simulation was however performed using this assumed characteristic for froth stability.

In Table 2, the simulated grades and recoveries at the default and peak values are compared. The first row shows the default froth depths and aeration rates as was reported by Harris (2000). The second row shows the results of using the same default froth depths, but using aeration rates where the stability peaks occur. The third and fourth rows were simulated with 20% deeper and 20% shallower froth levels than in the default case, and also using aeration rates corresponding with the peaks in froth stability.

This table provide some interesting figures that would need to be verified in an industrial application. A deeper froth is typically associated with a higher grade (and lower recovery), and high aeration rates with high recovery and lower grades. The aeration rates where the peak in froth stability occurs in a shallow froth, is however lower than

Table 2. Grade and recovery at default and peak α values

h_{froth}	J_g	Grade	Recovery
7.8 cm	Default	59.21	0.7904
7.8 cm	Peak	80.88	0.7338
9.4 cm	Peak	82.20	0.7245
6.3 cm	Peak	83.45	0.7294

in a deep froth, as was confirmed by (Hadler et al., 2012) on an industrial installation. For this simulation study, the combination of a deeper froth and higher aeration rate at the peak, resulted in a lower grade than what was achieved in a shallower froth. This can be explained by the higher overall froth stability at shallower froths, shown in Fig. 2. It confirms that a control strategy simply increasing froth depth and decreasing aeration rates are unlikely to operate at an optimum point.

For an industrial product, a minimum grade specification needs to be met, and typically no benefit is provided by delivering a higher specification product. An optimal operating point would thus still have to produce a product with the same grade as the default operation (59.21), but at a higher recovery. An optimisation strategy could potentially be used to find this point, but to illustrate the concept, a series of grade and recovery values at different froth depths and their peak values are shown in Table 3.

Table 3. Search for optimum grade and recovery at peak α values

h_{froth}	J_g	Grade	Recovery
7.8 cm	Default	59.21	0.7904
9.4 cm	Peak	82.20	0.7245
11.7 cm	Peak	82.3	0.7120
3.9 cm	Peak	79.95	0.7363
0.8 cm	Peak	78.5	0.698
0.4 cm	Peak	79.9	0.647
0.16 cm	Peak	61.4	0.665

It is clear from the values in Table 3 that the low default grade cannot be achieved at a viable froth depth when operating at a peak in froth stability. It is however still likely that operation can be improved by operating closer to the aeration rate peaks - even if not at the peaks. This test hence remains inconclusive, despite the significant increase in grade achieved at the peak froth stability points.

The reason for the large improvements in grade when operating at the peak froth stability values, is best illustrated by examining the grade and recovery curves for the default froth depths (7.8 cm) and a 50% shallower froth (3.9 cm), shown in Fig. 3 and 4. When J_g is operated at roughly 0.23 cm/s, large gains in grade can be made by operating at the peak froth stability point, without sacrificing significant recovery. This is however likely to be a difficult point to operate at in an industrial application, which may limit the usefulness of such an approach.

The grade-recovery curves at the default froth depth (7.8 cm) and a 50% shallower froth (3.9 cm) is shown in Fig. 5. As the curves intersect, the operating point dictates whether recovery would be higher or lower for the same grade, than what was achieved at the default operating point.

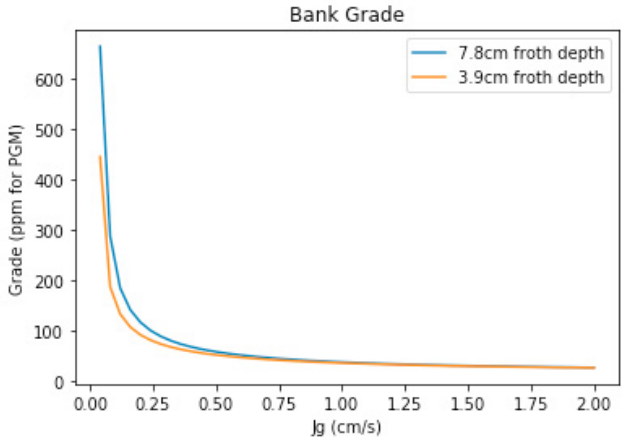

Fig. 3. Overall concentrate grade for flotation bank

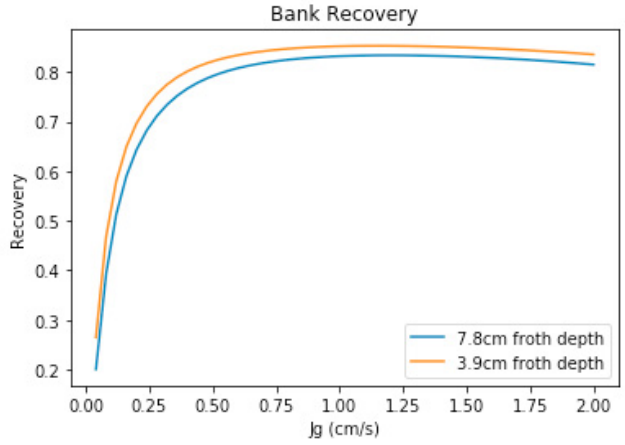

Fig. 4. Overall concentrate recovery for flotation bank

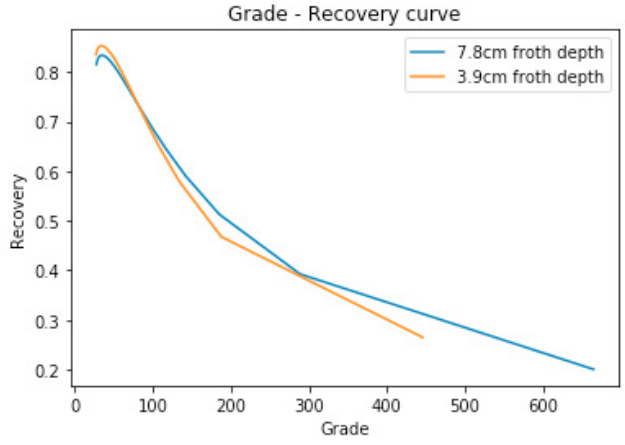

Fig. 5. Flotation bank grade-recovery curves

The inability to find an operating point at peak aeration rates, resulting in the same grade, but a higher recovery, prompted further investigation into the relative contributions of the empirical froth stability model compared to the rest of the fundamental flotation model. Froth stability is not the only factor that could improve recovery without sacrificing grade. The trade off in recoveries from true flotation and entrainment, which affects both the valuable mineral and gangue minerals, can also be used to increase the recovery of a bank. Both entrainment and true flotation depend on the concentrations of minerals in each flotation cell, which in turn depends on the minerals flowing into the cell from an upstream flotation cell.

A comprehensive sensitivity analysis is outside the scope of this paper. An optimisation algorithm was used instead to find an operating point of the same or higher grade as the default operating point, with an objective of maximising recovery. This algorithm was implemented on a model including a variable froth stability factor, and compared to a model with a constant froth stability factor. The improvement in bank recovery, and the change in operating points are given in Table 4.

For the model with a variable stability factor, the optimum was found at a reduced mean aeration rate (closer to the peak in froth stability) and lower froth depth, while the model with the constant stability found an optimum at a higher mean aeration rate and froth depth. This highlights the importance of having a fundamental froth stability model aligned with the underlying stability mechanisms. Although the different flotation mechanisms and their gains at different mineral concentrations can be used to optimise operation, froth stability plays a significant role that cannot be ignored.

Table 4. Comparisson of models with a fixed and variable froth stability factor

Model	Delta Recovery	Mean Aeration Rate	Mean Froth Depth
Variable Alpha	0.19%	-4.7%	-20.6%
Constant Alpha	0.07%	+2.4%	+5.9%

5. DISCUSSION

In order to optimise flotation operation, one needs to model the non-linearities in the process and develop control strategies to exploit these aspects of the flotation mechanisms. Most models that are currently used in flotation control assumes linear characteristics, which implies that the optimum will be located at a maximum or minimum limit. This explains why flotation control / optimisation strategies often attempts to control grade as close as possible to its minimum specification in order to maximise recovery.

As Neethling and Brito-Parada (2018) pointed out, reliable models – particularly for the froth phase, which are suitable for controller implementations are not available. While empirical models could provide benefit over a limited control range and in a simulation study, their applicability in industrial applications have not been proven, and the results presented may not provide an accurate representation of the extent of non-linearities in industrial applications. The froth phase is however a key component of the flotation process, and optimisation of the flotation process relies on the availability of reliable models.

In this study, the potential benefit of being able to track peak froth stability points by using a model was illustrated. A control strategy just exploiting the trade-off between grade and recovery would have been able to achieve the desired grade, but it is unlikely that it would have found an true optimum in a non-linear system.

Although this study is based on simulations, and uses a very simple model, the results are encouraging. It also showed how the interaction between froth depths and aeration rates can be used to optimise flotation operation. The challenge remains to either find a reliable fundamental model for froth stability, or alternatively a reliable method of updating an empirical model continuously with real-time data.

6. CONCLUSION

Flotation froth behaviour is a key aspect of flotation optimisation. All factors contributing to overall flotation performance are impacted by variations in froth stability, making any model that does not take froth characteristics into account only valid over a limited operating range. Although only minor gains in flotation performance was demonstrated, these were based on a closely monitored pilot plant configuration, and it is expected that significantly larger benefits can be achieved by including froth dynamics into a flotation optimisation strategy on industrial sites.

REFERENCES

Ata, S. (2008). Coalescence of bubbles covered by particles. *Langmuir*, 24(12), 6085–6091.

Bascur, O. and Herbst, J. (1985). On the development of a model-based control strategy for copper ore flotation. In E. Forsberg (ed.), *Flotation of Sulphide Minerals*, 409–431. Elsevier, Netherlands.

Hadler, K., Greyling, M., Plint, N., and Cilliers, J.J. (2012). The effect of froth depth on air recovery and flotation performance. *Minerals Engineering*, 36-38, 248–253.

Harris, T. (2000). *The Development of a Flotation Simulation Methodology Towards an Optimisation Study of UG2 Platinum Flotation Circuits*. Ph.D. thesis, University of Cape Town.

Laurila, H., Karesvuori, J., and Tiili, O. (2002). *Strategies for Instrumentation and Control of Flotation Circuits*, volume 1, 2174–2195.

Neethling, S.J. and Brito-Parada, P.R. (2018). Predicting flotation behaviour The interaction between froth stability and performance. *Minerals Engineering*, 120(February), 60–65.

Neethling, S.J. and Cilliers, J.J. (2009). The entrainment factor in froth flotation : Model for particle size and other operating parameter effects. *International Journal of Mineral Processing*, 93(2), 141–148.

Neethling, S.J., Lee, H.T., and Cilliers, J.J. (2003). Simple relationships for predicting the recovery of liquid from flowing foams and froths. *Minerals Engineering*, 16(11), 1123–1130. doi:10.1016/j.mineng.2003.06.014.

Oosthuizen, D.J., Craig, I.K., Jämsä-Jounela, S.L., and Sun, B. (2017). On the current state of flotation modelling for process control. *IFAC-PapersOnLine*, 50(2), 19–24.

Oosthuizen, D.J. and Craig, I.K. (2018). Flotation modelling based on floatability distributions regressed from routine data. *IFAC-PapersOnLine*, 51(21), 105–110.

Polat, M. and Chander, S. (2000). First-order flotation kinetics models and methods for estimation of the true distribution of flotation rate constants. *International Journal of Mineral Processing*, 58, 145–166.

Runge, K. and Franzidis, J.P. (2003). Structuring a flotation model for robust prediction of flotation circuit performance. *XXII International Mineral Processing Congress*, (October), 973–984.

Tang, J.A. and Tan, B.S. (1989). The Effect of Silica Oxide Particles upon Stabilization of Foam. *Journal of Colloid and Interface Science*, 131(2), 498–502.

Wang, L., Peng, Y., and Runge, K. (2016). Entrainment in froth flotation : The degree of entrainment and its contributing factors. *Powder Technology*, 288, 202–211.

Wills, B.A. and Napier-Munn, T. (2006). *Mineral Processing Technology:An Introduction to the Practical Aspects of Ore Treatment and Mineral Recovery*. October.

Zheng, X., Franzidis, J.P., and Johnson, N.W. (2006). An evaluation of different models of water recovery in flotation. *Minerals Engineering*, 19(9), 871–882.